

Suppression of Hepatitis B Virus X Protein-Mediated Tumorigenic Effects by Ursolic Acid

Hong-Yin Wu,[†] Chi-I Chang,[†] Bo-Wei Lin,[†] Feng-Ling Yu,[‡] Ping-Yuan Lin,[§] Jue-Liang Hsu,[†] Chia-Hung Yen,^{||} Ming-Huei Liao,[⊥] and Wen-Ling Shih^{*,†}

[†]Graduate Institute of Biotechnology, [⊥]Department of Veterinary Medicine, ^{||}Department of Life Science Pingtung University of Science and Technology, Pingtung, Taiwan

[§]Graduate Institute and Department of Life Science, Tzu-Chi University, Hualien, Taiwan

[‡]Department of Nursing, Tzu-Hui Institute of Technology, Pingtung, Taiwan

ABSTRACT: This study investigated the potential effects of natural products ursolic acid (UA) and oleanolic acid (OA) against HBx-mediated tumorigenic activities *in vitro* and *in vivo*. HBx transactivated Sp-1 and Smad 3/4 in Huh7 and FL83B hepatocytes and induced cell migration of Huh7 and HepG2. HBx also induced MMP-3 secretion in Huh7 and acted against TGF- β -induced apoptosis in Hep3B. UA almost completely blocked the HBx-mediated effects, while OA had a partial inhibitive effect. Utilization of specific MAPK inhibitors and immunoblotting demonstrated that UA selectively activated MAPK signaling in certain tested cells. Preintra-peritoneal injection of UA fully prevented the tumor growth of HBV-containing 2.2.15 cells, while OA-treated mice had smaller tumors than the control group. Our results suggested that UA possesses a hepatoprotective ability and illustrated the evident effects against HBx-mediated tumorigenic activities without toxicity in a mouse model.

KEYWORDS: HBx, ursolic acid, hepatoprotective, MAPK

INTRODUCTION

Long-term epidemiological study, animal experiments and molecular biology research have confirmed that chronic hepatitis B virus (HBV) infection is the major cause of liver cancer.¹ Although the hepatitis B virus (HBV) vaccine and preventative measures have been implemented for many years,² the numbers of new infections and chronic carriers of HBV and the incidence of liver cancer are still rising, possibly due to the existence of HBV mutants,³ drug-resistant virus strains,⁴ or vaccine non-responders.⁵ Thus, HBV remains a serious health threat in many countries worldwide.

Hepatitis B virus X protein (HBx) contains 154 amino acids and has long been suspected to play critical and multiple roles in the pathogenesis of hepatocellular carcinoma development⁶ based on its tumorigenic activity *in vitro* and *in vivo*.⁷ HBx modulates the function of host factors through direct interaction or indirect mechanisms, including cellular factors involved in intracellular signaling pathways, apoptosis regulators, nucleus transcriptional factors and regulators, and protein degradation machinery, as well as DNA damage response regulators.⁸ Investigations have used different cell culture systems, different expression strategies (for example, transient higher-level, long-term lower-level or inducible expression) and different detection methods, and some results have been controversial.⁸

The results of animal model studies and clinical trials have confirmed that many natural plant ingredients have a considerable preventative effect against cancer. At present, more than 2000 natural ingredients have been tested and reported to have a significant inhibitive effect on cancer, and the strategy of using combinations of multiple ingredients is being employed in clinical trials on a large scale. Some studies have demonstrated

that the strategy can be used at any stage of tumor progression and has been shown to inhibit tumor growth or even destroy tumor cells.⁹ However, the mechanisms of tumor inhibition of these effective natural ingredients are mostly unknown; furthermore, some of these natural compounds may exert a cytotoxic effect, and the treatment efficacy needs to be confirmed using an *in vivo* approach.¹⁰

Ursolic acid (UA) and oleanolic acid (OA) are pentacyclic triterpenoid acids that are widely distributed in medical herbs and other plants in the form of free acid or aglycons.¹¹ Both have been demonstrated to possess antioxidative,¹² anti-inflammatory,¹³ antitumorigenesis,¹⁴ and antiangiogenesis¹⁵ properties in cell cultures and animal studies. Similar to tangeretin and nobletin, they act on cellular signaling pathways such as c-Jun N-terminal (JNK),¹⁶ PKC zeta,¹⁷ p53 and NF- κ B,¹⁸ as well as signal transducer and activator of transcription 3 (STAT 3),¹⁹ and so on, which are involved in cell cycle control, apoptosis regulation and tumor formation. Thus, UA and OA were investigated in terms of various parameters of HBx-mediated transcriptional activation, induction of cell migration and antiapoptosis in certain culture systems established by us, and were further examined to identify any tumor prevention ability in a mouse model.

MATERIALS AND METHODS

Cells and Transfection. Hepatoma cell lines Huh7, HepG2 and Hep3B were cultured in Dulbecco's modified Eagle medium (DMEM)

Received: December 3, 2010

Accepted: January 10, 2011

Revised: January 5, 2011

Published: February 11, 2011

containing 2 mM L-glutamine, nonessential amino acids, 1% penicillin and streptomycin mix, and 10% fetal bovine serum. For Hep3B pooled stable clones, complete DMEM additionally provided 500 $\mu\text{g}/\text{mL}$ G418. FL83B, normal hepatocyte cells from mice, were purchased from the Food Industry Research and Development Institute (Hsinchu, Taiwan) and were grown in Ham's F12 medium supplemented with the above antibiotics, L-glutamine and 10% fetal bovine serum. All cells were maintained at 37 °C under 5% CO₂. Transfection was performed using Lipofectamine 2000 (Invitrogen, Carlsbad, CA, USA) according to the user manual.

Reagents, Plasmids and Antibodies. TGF- β and silymarin were purchased from Sigma. UA and OA were prepared in the laboratory of a coauthor of this study, C.-I.C. Briefly, UA and OA were isolated from the leaves of *Morinda citrifolia* (Rubiaceae) after repeated column chromatography, and their structures were confirmed by comparing their ¹H NMR, ¹³C NMR and EI-MS spectral data with those of UA and OA (data not shown) described in the literature.²⁰ NMR spectra were recorded in CDCl₃ at room temperature on a Varian Mercury plus 400 NMR spectrometer, and the solvent resonance was used as the internal shift reference (TMS was employed as the standard). PD98059, SP600125 and SB203580 were purchased from Calbiochem (San Diego, CA, USA). Luciferase reporter Sp-1-Luc and Smad 3/4-Luc are commercially available plasmids (Panomics, Redwood City, CA, USA) that contain a specific transcription factor binding consensus sequence upstream on the luciferase gene. Mammalian expression vector RC/RSV containing RSV promoter and G418 selection marker was used for HBx expression. All transfected DNA were prepared using Qiagen Maxi-prep purification columns (Qiagen, Valencia, CA, USA). Antibodies against GAPDH were purchased from Santa Cruz Biotechnology (Santa Cruz, CA, USA); other antibodies were obtained from Cell Signaling Technology (Beverly, MA, USA). HBx detection employed an antibody generated in our laboratory by immunizing rabbits with *Escherichia coli* expressed HBx.²¹ Secondary antibodies conjugated with horseradish peroxidase (HRP) were obtained from GE Healthcare (Piscataway, NJ, USA).

BrdU Incorporation for Cell Proliferation Quantification. Cell proliferation ELISA was purchased from Roche, and the experiment was performed according to the manufacturer's instructions. Briefly, the serially diluted 4 compounds were added to 96 wells containing cultured cells and the medium and compounds were changed every 3 days. The cell proliferation status was measured every day. Before measurement, cells were labeled with BrdU using a kit for 4 h at 37 °C and FixDenat solution was then added, followed by incubation at room temperature for 30 min. Antibodies labeled with peroxidase against BrdU were then added and incubated, followed by washing and substrate addition. Chemiluminescence was measured using a luminometer (Turner Biosystem), and for calculation of the IC₂₀ and IC₅₀ compound concentrations, the data were plotted on a semilog scale and values were determined by graphic analysis.

Luciferase Assay. Cultured cells were cotransfected with the indicated reporter plasmids and HBx expression plasmid RSV/HBx or control vector RC/RSV together with pRKbetaGAL plasmid containing CMV promoter upstream of the β -galactosidase gene and then incubated for various experimental time periods. Compounds were subsequently pretreated, followed by DNA transfection. Luciferase and β -galactosidase activity were determined using a Luciferase assay system and a β -galactosidase enzyme assay system (Promega, Madison, WI, USA), respectively. Luciferase activity was normalized to β -galactosidase activity to account for the transfection efficiency. Luciferase activity was measured using a luminometer (Turner Biosystem), while β -galactosidase activity was measured using a model 680 Microplate reader (Bio-Rad, Richmond, CA, USA).

Cell Migration Assay and MMP-3 Secretion. Cell migration was assayed using a Transwell culture insert (Becton, Dickinson, Franklin Lakes, NJ, USA). Cells were seeded in the top part of the

Transwell insert, and after incubation the cells on the upper filter were removed using a cotton swab then stained with crystal violet. The migratory cells were observed under a light microscope operating at 200 \times magnification. To determine the secreted MMP-3 in the conditioned medium, ELISA (Amersham Biosciences, Buckinghamshire, U.K.) was performed.

Establishment of HBx-Expressing Hep3B Stable Clones. 70% confluent Hep3B cells cultured in a 10 cm dish were transfected with 20 μg of RSV/HBx and cultured for 48 h. For selection, 700 $\mu\text{g}/\text{mL}$ G418 was added to the medium for 2 weeks, following which all resistant cell clones were pooled, expanded and assayed for HBx expression by Western blotting analysis.

TUNEL Assay and Caspase-3 Activity Assay. A DNA fragmentation kit and a caspase-3 fluorescent assay kit were obtained from Clontech (Palo Alto, CA, USA). The precise experimental procedures were as per the user manual. For TUNEL assay, cells were washed with cold PBS and fixed using 4% formaldehyde at 4 °C for 30 min. After washing with PBS, cells were permeabilized with prechilled 0.2% Triton X-100. Cells, including a DNase-treated positive control sample, were then incubated with reaction mixture or a TdT-minus negative control mixture. The slides were incubated in the dark in a humidified incubator to perform the tailing reaction at 37 °C for 60 min. The apoptotic cells exhibited nuclear green fluorescence under a 520 nm filter. To measure the caspase-3 activity, cells were resuspended in chilled lysis buffer and cell lysates collected by centrifugation. Addition of reaction mixture and caspase-3 substrate was followed by incubation at 37 °C for 2 h. Fluorescence was read using a fluorometer (Turner Biosystem) at a 400 nm excitation with a 505 nm emission filter.

Ras Activity Assay. Ras activation assay was performed using a nonradioactive Ras-GTP assay (Upstate Biotechnology, Lake Placid, NY, USA) and a Ras ELISA assay (Upstate Biotechnology) according to the manufacturer's instructions. For the Ras activation assay, cultured cells were lysed with ice-cold Mg²⁺ lysis buffer. 10 μg of Raf-1 RBD (corresponding to the human Ras binding domain, residue 1 to 149 of Raf-1) agarose was added to 1 mg cleared lysates followed by incubation for 1 h at 4 °C with gentle rotation. The agarose beads were collected by brief centrifugation and after washing were then resuspended in Laemmli buffer and boiled. The supernatant was then loaded onto SDS-PAGE, and Western blotting analysis was performed using anti-Ras antibody. Only active Ras (Ras-GTP) binding to Raf-1 RBD was detected on the X-ray film. Recombinant Raf-1 RBD binds to the 96-well glutathione-coated ELISA plate, thus capturing the active-Ras of cell lysates prepared in the same way as for the Ras activation assay. Anti-Ras monoclonal antibody was then added, followed by incubation and washing and the subsequent addition of secondary antibody and the prepared chemiluminescent substrate.

Animal Experiments and Tumor Measurement. Three-week-old Nu/Nu mice were purchased from BioLasco (Taipei, Taiwan). All animal experiments were conducted following the guidelines of our university in accordance with the animal protection laws of Taiwan. Mice were kept for one week for environmental stabilization and observation of their general health. The mice were then randomly grouped into 9 groups, each containing 6 mice. The groups were as follows: nontreated negative control group, corn oil intraperitoneal injection and 2.2.15 cell subcutaneous inoculation group, UA and 2.2.15 cell-treated group, OA and 2.2.15 cell-treated group, silymarin combined with 2.2.15 cell inoculation group, and corn oil, UA, OA or silymarin injection groups. After one week, excluding the negative control, mice were injected with compound dissolved in corn oil every day at a dose of 50 mg/kg until the end of the experiment. After 7 days of injection, 10⁶ 2.2.15 cells in 100 μL of PBS were injected through the subcutaneous route in the applicable groups followed by compound injection until the 8-week point. All mice were then sacrificed and serum samples collected. Tumor diameters were also measured using electronic digital calipers.

Table 1. The IC₂₀ and IC₅₀ Values of the Various Compound Treatments on Hepatocyte and Hepatoma Cell Lines^a

cell line	ursolic acid (μM)		oleanolic acid (μM)	
	IC ₂₀	IC ₅₀	IC ₂₀	IC ₅₀
	7 Days			
FL83B	10.9 ± 0.7	17.8 ± 1.1	12.4 ± 1.3	20.1 ± 1.6
HepG2	10.5 ± 1.3	18.9 ± 0.9	11.4 ± 0.8	19.6 ± 1.4
Huh7	12.9 ± 1.0	18.4 ± 0.6	14.8 ± 0.6	20.3 ± 1.8
Hep3B	13.1 ± 1.0	19.4 ± 0.8	13.5 ± 0.4	19.1 ± 1.5
	14 Days			
FL83B	9.4 ± 0.9	16.9 ± 1.6	9.8 ± 1.6	18.9 ± 1.2
HepG2	9.8 ± 0.4	17.4 ± 0.8	9.3 ± 0.9	16.9 ± 1.1
Huh7	10.0 ± 0.7	16.5 ± 1.1	10.4 ± 0.8	19.6 ± 1.2
Hep3B	10.2 ± 0.6	16.9 ± 0.7	11.0 ± 1.0	17.8 ± 1.6

^aThe results are expressed as the mean and standard deviation of three independent experiments, each performed in duplicate.

Serum GOT, GPT, BUN and CRE Measurement. For examination of liver and renal function, the concentrations of GOT/GTP and blood urea nitrogen (BUN)/creatinine (CRE) in serum were measured by SPOTCHEM EZ sp-4430 (ARKRAY, Japan) using SPOTCHEM II GOT, GPT, BUN, and CRE Reagent Strips, respectively. Briefly, 10 μL of serum was automatically placed on the test field of the specific Reagent Strip, which then permeated into the reagent layer, where the reaction occurred. GOT or GPT in the serum transferred the amino group of L-alanine or L-aspartic acid to α -ketoglutaric acid and produced L-glutamic acid and pyruvic acid or oxalacetic acid, respectively; the oxalacetic acid generated pyruvic acid by oxalacetic decarboxylase, and the pyruvic acid was then oxidized by the pyruvic acid oxidase to produce hydrogen peroxide, which oxidized and condensed 4-aminoantipyrine and N-ethyl-N-(2-hydroxy-3-sulfopropyl)-3,5-dimethoxyaniline sodium salt by the peroxidase to form a blue color, measured at 610 nm. The rate at which the blue color is generated in this detection layer is proportional to the GOT or GPT activity in the serum, respectively. Urea in the serum reacted with o-phthalaldehyde to produce 1,3-dihydroxyisoindoline, which reacted with N-1-naphthyl-N'-diethylethylenediamineoxalic acid to form a blue–purple color, measured at 610 nm. The rate at which the blue–purple color is generated in this detection layer is proportional to the concentration of blood urea nitrogen in the serum. Creatinine in the serum reacted with 3,5-dinitrobenzoic acid to form a red color measured at 550 nm, and the intensity of the red color as determined by reflectance spectrophotometry is proportional to the concentration of creatinine in the serum.

Statistical Analysis. The statistical significance was calculated by Student's *t* test using the software SigmaPlot Scientific Graph System (Jandel Scientific, San Rafael, CA). **P* values of <0.01 were considered to be statistically significant. The results are shown as the mean and standard deviation. All data were obtained by performing three independent experiments, each in duplicate.

RESULTS

Cytotoxicity of Nobiletin, Tangeretin, Ursolic Acid and Oleanolic Acid toward Hepatocyte and Hepatoma Cell Lines. It was confirmed that the concentration of the compounds used did not impair cell growth. Chemiluminescence immunoassay was performed for direct quantification of cell proliferation based on the measurement of 5-bromo-2'-deoxyuridine (BrdU) incorporation during DNA synthesis. To ensure that the compounds did not influence cells long-term, cell

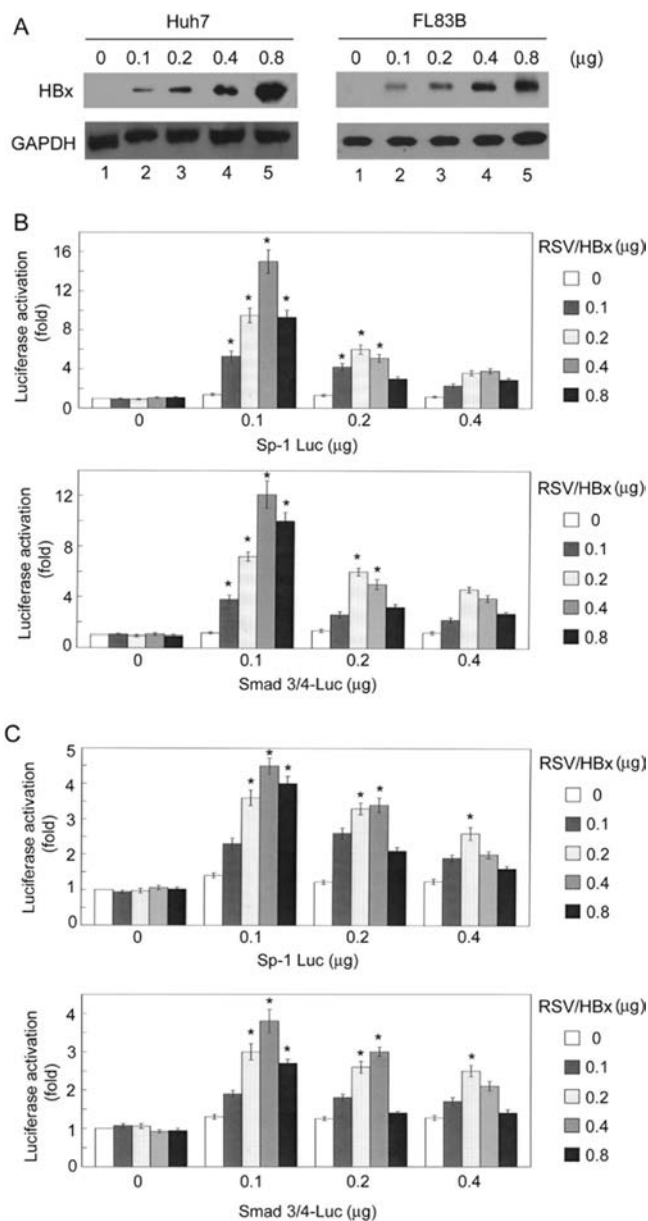


Figure 1. Detection of HBx expression and HBx-mediated transcriptional activation. (A) Cultured cells in 24-well plates were transfected with HBx expression plasmid RSV/HBx in differing amounts and incubated for 48 h. Total cell lysates were then collected and subjected to Western blotting using anti-HBx antibody. GAPDH was included as an internal loading control. Luciferase assay was performed in Huh7 (B) and FL83B (C). Cultured cells were cotransfected in 24-well plates with the indicated amounts of luciferase reporter and HBx expression plasmid together with 20 ng of pRKbetaGAL and then incubated for 48 h. Luciferase and β -galactosidase activities were measured. All data represent the mean and standard deviation of the luciferase activation fold after normalization to β -galactosidase activity. Three independent experiments were performed, each in duplicate. * indicates a significant difference compared with cells without reporter and effector DNA.

proliferation was measured every day for 14 days, and the IC₅₀ and IC₂₀ were calculated as shown in Table 1. To avoid cytotoxicity-induced side effects, we deliberately utilized 9 μM ursolic acid and oleanolic acid for further experiments, the used concentration being lower than the IC₂₀ after 14 days treatment. Additionally, proving that the concentrations of the

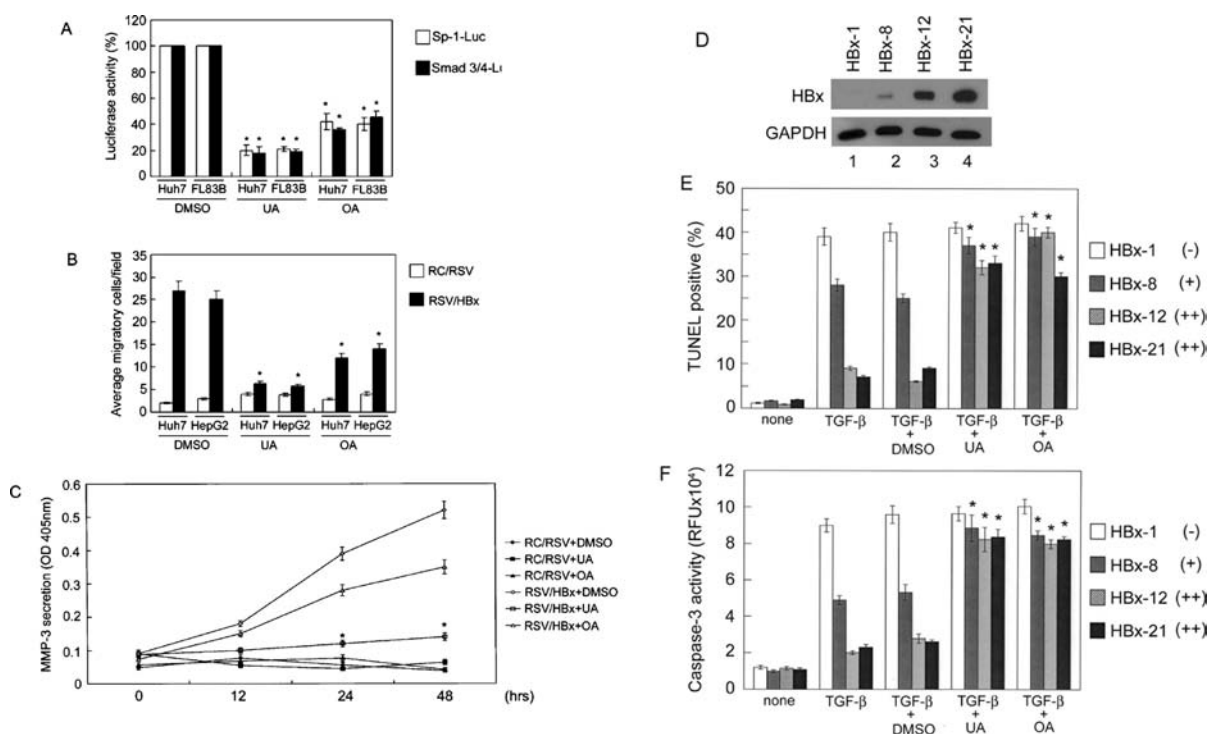


Figure 2. UA and OA released HBx-mediated effects. Cultured cells in 24-well plates were pretreated with the selected compound for 4 h and the subsequent experiments were then performed as follows. (A) Luciferase assay. Huh7 and FL83B were cotransfected with RSV/HBx 0.4 μ g and reporter plasmid 0.1 μ g then incubated with compound for an additional 48 h. (B) Cell migration assay. Cells were transfected with the indicated plasmid 0.5 μ g for 24 h, and then 2×10^4 transfected cells were seeded onto the upper side of the Transwell culture insert. The cells migrating across the filter were stained and counted in 20 independent fields. The *y*-axis represents the average migratory cell number per $200\times$ field. (C) MMP-3 secretion assay. The levels of secreted MMP-3 in various treated Huh7-conditioned media were determined. Twenty-four wells of Huh7 were pretreated with DMSO or compound then transfected with the indicated plasmid 0.5 μ g, followed by incubation for different durations. The OD405 nm was proportional to the secreted MMP-3 level and is shown on the *y*-axis. The above experiments were performed thrice independently in duplicate. (D) Western blotting analysis. Different expression levels of selected pooled RSV/HBx-transfected Hep3B cells. (E) TUNEL assay. Parental Hep3B, selected Hep3B cells treated with 5 ng/mL TGF- β for 24 h, or cells pretreated with undecated compound for 4 h followed by 5 ng/mL TGF- β for an additional 24 h. The TUNEL positive percentage demonstrated the average apoptotic cell ratio of 10 fields at $200\times$ magnification. (F) Caspase-3 activity assay. The same experimental design and treatment as described in Figure 2E were used. The *y*-axis represents caspase-3 activity. The significant difference was in comparison with DMSO-treated cells.

used compounds did not impair cell growth, identical cell phases were demonstrated by flow cytometry under our selected compound treatments (data not shown).

HBx-Mediated Transcriptional Activation. HBx expression in our system was confirmed in a dose-dependent manner on human hepatoma Huh7 cells and normal mouse hepatocyte FL83B cells (Figure 1A). Luciferase assay showed that HBx transactivates Sp-1 and Smad 3/4 in Huh7 (Figure 1B) and FL83B (Figure 1C) to differing degrees. We suspected that the different cellular contents of hepatoma and hepatocytes resulted in the transactivation fold being higher in Huh7 cells. Importantly, the transcriptional activation pattern revealed that a critical effector and reporter ratio of 4:1 resulted in the best transactivation level. Other reporters including p53-Luc and AP-1-Luc were unable to be induced in the presence of HBx in Huh7, FL83B and HepG2 (data not shown). However, without HBx expression, only transfection of NF- κ B-Luc into Huh7 and HepG2 resulted in increased and dose-responsive luciferase activity; thus, we excluded these three reporters in our further experiments.

Suppression of HBx-Induced Tumorigenic Effects by UA. Having confirmed that HBx selectively transactivates Sp-1 and Smad 3/4, we further examined the HBx-mediated effects of UA

and OA, including transcriptional activation and hepatoma cell migration induction,²² against TGF- β -induced apoptosis,²¹ which we had established previously. The results shown in Figure 2A demonstrated that UA and OA significantly reduced HBx-induced Sp-1 and Smad 3/4 activation in Huh7 and FL83B cells, while UA revealed a better repressive ability than OA. HBx expression elicited hepatoma cell migration in both Huh7 and HepG2 cells and increased matrix metalloproteinase-3 (MMP-3) secretion,²² while Huh7 and HepG2 cells pretreated with UA and OA demonstrated cell migration and MMP-3 release, and UA had a better inhibition activity than OA (Figure 2B and 2C). To evaluate the influence of the tested compounds on the HBx-mediated antiapoptosis function, HBx-expressing Hep3B stable clones with or without differing levels of expression of HBx (Figure 2D) were used to study the effects of the natural compounds on TGF- β -induced apoptosis. Cells treated with TGF- β alone and cells pretreated with the natural compounds followed by addition of TGF- β were compared. TUNEL assay and caspase-3 activity assay indicated that cells with higher HBx expression had a better antiapoptotic activity (Figure 2E and 2F, second and third groups). In the presence of UA and OA, the apoptotic cell and caspase-3 activities were dramatically reversed (Figure 2E and 2F, sixth and seventh groups).

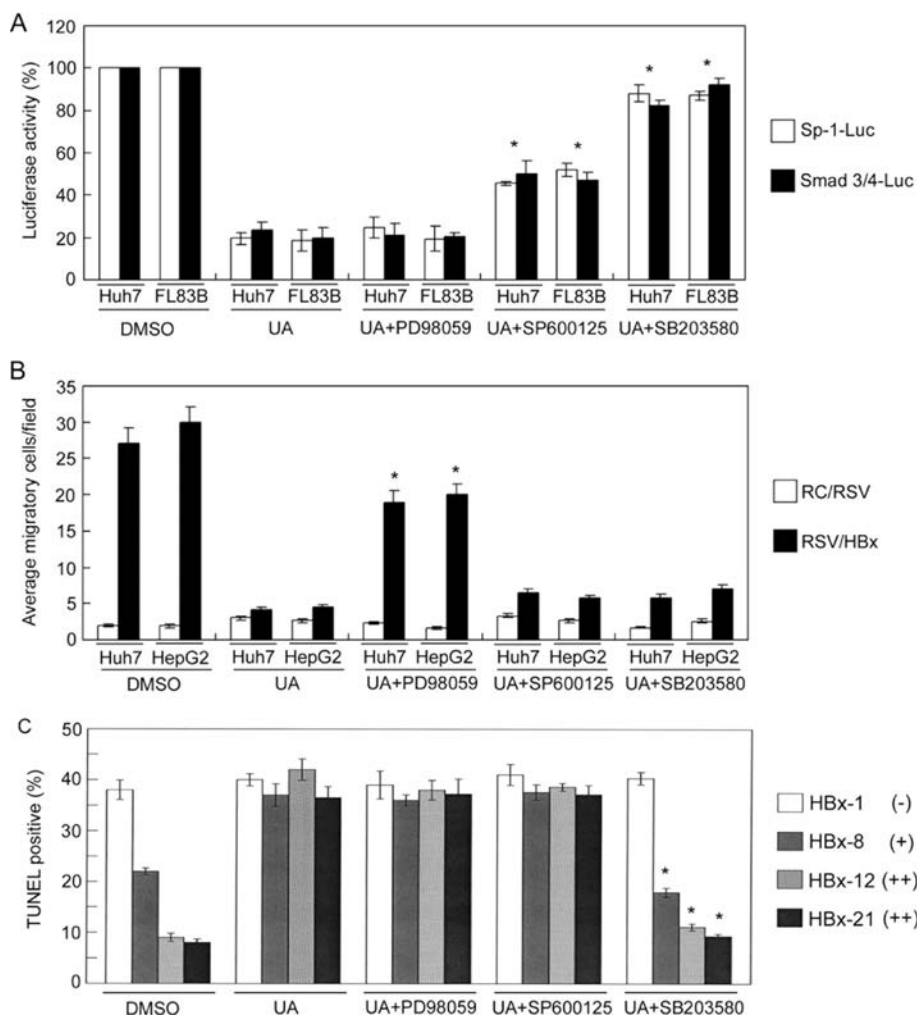


Figure 3. Roles of ERK, JNK and p38 MAPK in the UA-mediated effect. Cultured cells were pretreated with a single or two compounds as indicated for 4 h. Subsequently, cells were subjected to luciferase assay, as shown in Figure 2A (A), cell migration assay, as shown in Figure 2B (B), or TUNEL assay, as shown in Figure 2E. The significant difference was in comparison with UA-treated cells.

Selective Involvement of MAPK Signaling in UA-Induced Suppression of HBx-Mediated Tumorigenic Effects. We next evaluated the possible involvement of MAPK signaling pathways by using specific inhibitors PD98059, SP600125 and SB203580, which blocked extracellular signal-regulated kinase-1 (ERK-1),²³ JNK²⁴ and p38,²⁵ respectively. The working concentrations of the various inhibitors were 20 μ M PD98059, 10 μ M SP600125 and 5 μ M SB203580, which were not deleterious to the cells, as determined by measurement of a sensitive marker, lactate dehydrogenase activity (LDH), and Brdu incorporation (data not shown). SP600125 and SB203580 both reversed the UA-mediated suppression effect in HBx-induced transactivation, while SB203580 showed the better effect (Figure 3A), suggesting critical roles of JNK and p38 signaling in UA-mediated activity. In a cell migration assay, only PD98059 significantly reversed the UA-mediated activity (Figure 3B), indicating the important function of ERK signaling in cell migration. Finally in the Hep3B cell system, treatment with p38 inhibitor SB203580 released the UA-mediated activity against HBx-induced antiapoptosis activity (Figure 3C). The results for caspase-3 activity were identical (data not shown), as demonstrated by TUNEL assay, which confirmed the involvement of p38 signaling transmission in this system.

Activation of MAPK Signaling Molecules by UA. Having demonstrated the selective involvement of ERK, JNK and p38 in UA-mediated activities, further experiments were performed to analyze the status of the upstream MAPKK and MAPK and downstream transcription factor ATF-2 based upon the results shown in Figure 3. Figure 4A shows that, after treatment of Huh 7 with UA for different periods of time, the phosphorylation levels increased with differing kinetics, including those of c-Raf (panel 1), ERK 1/2 (panel 5) and ERK upstream activator MEK 1/2 (panel 3), p38 (panel 9) and p38 upstream activator MKK 3/6 (panel 7), JNK (panel 13) and JNK upstream activator MKK 4/7 (panel 15), and the downstream transcription factor ATF-2 (panel 15). The total expression level was not altered (Figure 4A, even panels). In FL83B cells treated with UA, the phosphorylation levels of p38, JNK and their upstream activator MKK 3/6 and MKK 4/7, as well as ATF-2, were gradually upregulated and then declined (Figure 4B, odd panels). Similar and expected results were observed for HepG2 (Figure 4C) and Hep3B cells (Figure 4D). Treatment of Huh7 and HepG2 cells with UA induced c-Raf phosphorylation, which led us to further evaluate the Ras status of these two cell lines. Upon UA and OA treatment, Ras activity ELISA (Figure 4E) and active Ras pull-down assay (Figure 4F) showed that UA and OA activated Ras in

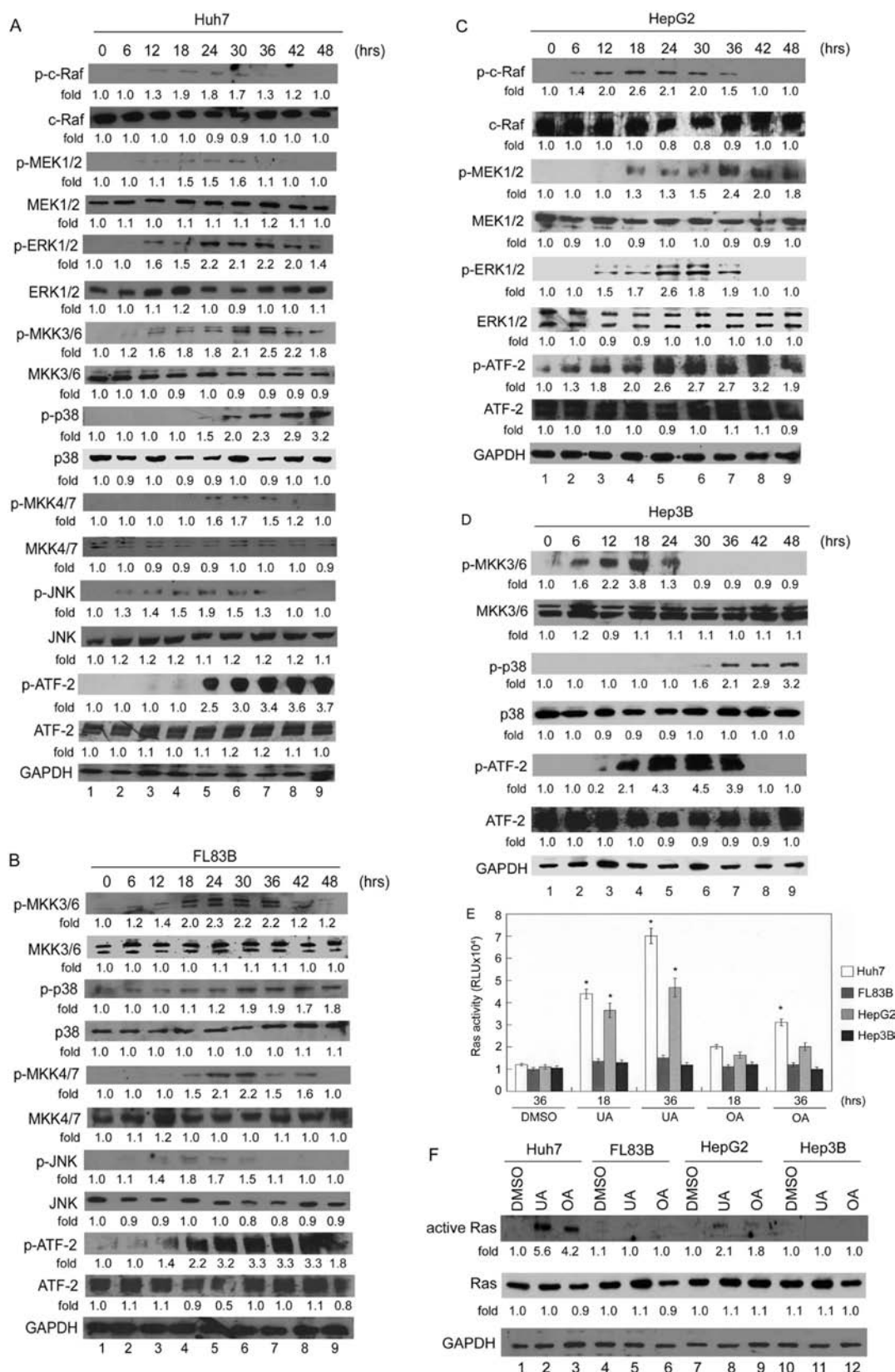


Figure 4. Activation of MAPK signaling pathway. (A–D) Cultured cells were treated with UA for various periods of time. A 40 μ g soluble protein sample was subjected to Western blotting analysis using antibodies against MAPK signal molecules, as shown. (E) Ras ELISA activity assay. Indicated cells were treated with UA or OA for 18 or 36 h; Ras activity is shown on the y-axis, and the significant difference is in comparison with DMSO-treated cells. (F) Ras activation assay. Cells were treated with UA or OA for 36 h; active Ras is shown. The Western blot signals were further quantified and are shown as fold induction using Syngene quantification system software (Frederick, MD, USA).

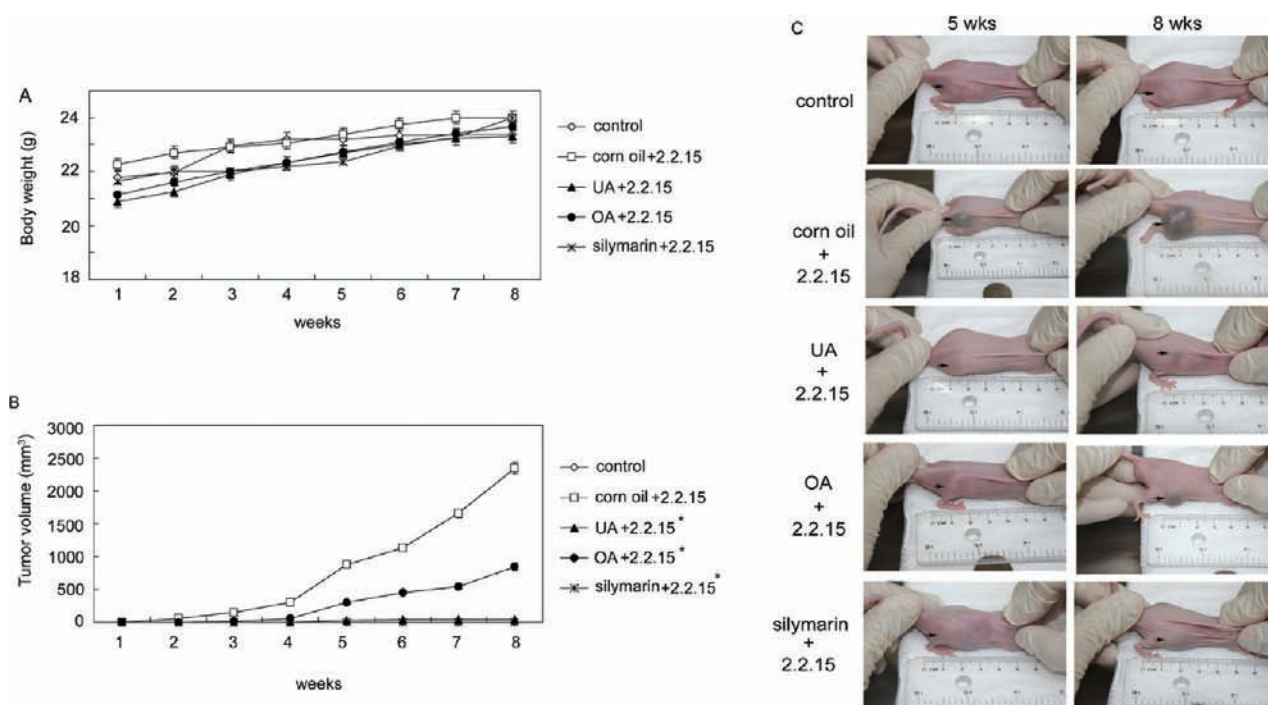


Figure 5. Animal experiments. After one week of acclimatization, mice were subjected to compound injection. The *x*-axis shows the time course after 2.2.15 inoculation. Control represents the no-treatment mice. (A) Average mouse body weight during the 8-week experiment. (B) Average tumor volume was measured by the Vernier scale. The UA-, OA- or silymarin-treated mice showed significant differences in tumor volume as compared with corn oil-treated mice. (C) After 5 and 8 weeks of 2.2.15 inoculation; the cell injection site is indicated by the arrow.

Huh7 and HepG2, and not in Hep3B and FL83B, while OA partially induced Ras activity. DMSO-treated Huh7, FL83B, HepG2 and Hep3B cells for the same time period did not alter the protein phosphorylation and expression levels (data not shown). Thus, the results shown in Figure 3 and Figure 4 together confirmed that UA elicited Ras-Raf-MEK1/2-ERK1/2, MKK 3/6-p38 and MKK 4/7-JNK signaling transmission selectively in our cells; ERK, JNK and p38 activation in Huh7 upon UA treatment; JNK and p38 activation in FL83B; Ras-Raf-MEK 1/2-ERK1/2 activation in HepG2; and p38 activation in Hep3B cells. At the higher UA concentration of 15 μ M, 25% significant cell death was observed at 24 h post-treatment, although certain molecules could be activated (data not shown).

UA Prevents HBV-Containing-Cell-Induced Tumor Formation in a Mouse Model. Nu/Nu mice were employed to evaluate the effect of UA on HBV-containing hepatoma formation. Three-week-old Nu/Nu mice were purchased and allowed to acclimatize for one week. They were then split into groups, each group containing 6 mice. The mice were then injected with only corn oil, 50 mg/kg UA, OA, or a well-known hepatoprotective compound silymarin²⁶ as the positive control, or test compound followed by 2.2.15 cells expressing all HBV proteins, including HBx.²⁷ Before subcutaneous injection of HBV-containing 2.2.15 cells,²⁸ corn oil or the different natural compounds were preinjected *via* the peritoneal cavity every day for one week, and were continuously subsequently injected for 8 weeks. During the 8 weeks of observation, no significant changes in body weight were observed in the mice under the different treatments (Figure 5A). In addition, their activity in terms of food ingestion and excretion was almost no different between groups based on our observations (data not shown). The sizes of the tumors in each group were measured every week, and the results were as

shown in Figure 5B. The control group represented normal mice without any treatment. In the 2.2.15 cell-inoculated group, the 6 mice injected with corn oil all developed tumors of an average size of greater than 2000 mm³ (Figure 5B and 5C, second panel), while the silymarin-treated mice did not grow tumors (Figure 5B and 5C, fifth panel), which confirmed its tumor-preventive activity. In the UA-treated mice, 5 of the 6 mice did not grow tumors, while one mouse had a small tumor of about 80 mm³ (Figure 5B and 5C, third panel). In the OA-treated mice, 3 of the 6 mice grew tumors of an average size of 780 mm³ at the eighth week (Figure 5B and 5C, fourth panel). No body weight change or tumor formation was observed in mice treated with corn oil, UA, OA or silymarin (data not shown). Mice experiments using with 200 mg/kg compound administration, as described above, showed identical tumor prevention capacity (data not shown).

UA and OA Lowered Liver Damage and Did Not Affect Liver and Renal Function. To evaluate the effects of long-term usage of the tested compounds, mice serum samples were collected after 9 weeks of compound injection, and conventional liver function markers, glutamino-oxaloacetic transaminase (GOT) and glutamino-pyruvic transaminase (GPT),²⁹ were examined. In comparison with the nontreated control group, the 2.2.15-cell-inoculated mice had elevated serum levels of GOT and GPT (Figure 6A, the first two groups). UA treatment lowered the GOT and GPT levels significantly, while OA had only a partial effect and silymarin had the best effect (Figure 6A, third to fifth groups). In mice treated with corn oil and a single compound only for 9 weeks, the GOT and GTP levels were comparable (Figure 6A). Blood urea nitrogen (BUN) and creatinine (CRE) were assayed as typical markers of kidney function,³⁰ and all mice, including the negative controls, corn

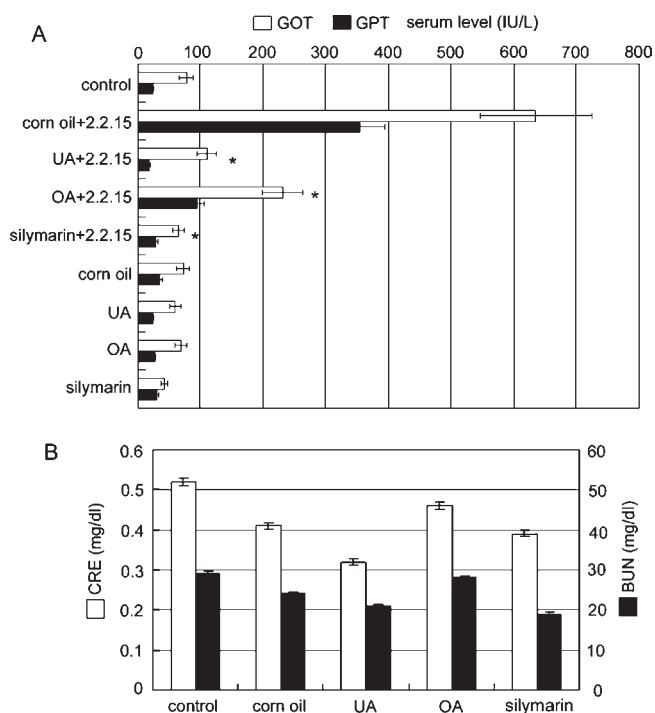


Figure 6. Effects of compound injection on liver and kidney function. (A) Average serum GOT and GPT levels. After the 8-week experiments, serum was collected from the different groups of mice. (B) Average serum BUN and CRE levels are shown on the two sides of the *y*-axis; the nontreated control, corn oil-, UA-, OA- and silymarin-treated mice are indicated on the *x*-axis.

oil-treated and compound-injected mice, exhibited comparable levels of BUN and CRE (Figure 6B).

DISCUSSION

The biological activities of HBx interact with the host cells through direct interaction or indirect mechanisms. Transcription is activated through direct binding to molecules regulating the transcription machinery, stimulating the MAPKs and JAK/STAT signaling pathways via indirect processes. Transcriptional activation is the most well-known function of HBx, and numerous transcription factors have been shown to be activated in the presence of HBx in a variety of cell culture systems. The related mechanisms and roles in hepatocarcinogenesis have been discussed in several review articles.⁶ HBx induces apoptosis³¹ or sensitized cells undergoing apoptosis³² in certain circumstances, and numerous studies have demonstrated the antiapoptosis activity of HBx.²¹ The accumulated evidence suggests that HBx plays a role in virus replication and might be a key component in the development of hepatocellular carcinoma.

UA and OA are triterpenoid compounds found in various plants that are widely used in traditional medicine. They have several important effects in the treatment of cancer, as they have been shown to possess antiangiogenic¹⁵ and antitumor activities³³ *in vitro* and *in vivo*. UA and OA have a similar structure, the only difference being the site of the methyl group on ring E, the distinctive methyl group being at C19 in UA and C20 in OA.³⁴ In the current study, UA had a notably greater effect than OA in the prevention of HBx-mediated tumorigenic activities in cultured hepatoma cells, including transactivation of Sp-1 and Smad 3/4 in Huh7 and hepatocyte FL83B, induction of

hepatoma cell migration, and MMP-3 secretion. This suggests that the methyl group plays a key role in determining the conformation that is associated with the biologic functions highlighted in this study.

UA and OA also inhibit TGF- β -induced apoptosis in Hep3B cells; however, tangeretin and nobletin do not alter the HBx-mediated carcinogenic activities. Like tangeretin and nobletin, UA and OA have been shown to play roles in the signaling pathways involved in tumor development, which include c-Jun N-terminal (JNK),¹⁶ PKC zeta,¹⁷ p53 and NF- κ B,¹⁸ and signal transducer and activator of transcription 3 (STAT 3).¹⁹ Recent studies have shown that UA modulates MAPK signaling and has an influence on apoptotic cell death.³⁵ When inhibitors of MEK, JNK and p38 were employed to validate the involvement of the MAPK signaling pathways in the HBx-mediated tumorigenic effect, the results demonstrated that JNK inhibitor SP600125 and p38 inhibitor SB203580 reversed the UA-mediated suppression of HBx transactivation, the effect of SB203580 being more evident, suggesting that the p38 pathway is more important. On the other hand, MEK is not associated with this process, as PD98059 has no effect on the suppression of the HBx-induced tumorigenic effect by UA. In addition, with regard to the hepatoma cell migration suppressed by UA, the MEK pathway is important; however, the JNK and p38 pathways have no effect on the event. In the analysis of the expression of MAPK signaling molecules in different human hepatoma cell lines and normal mouse hepatocytes, we demonstrated that UA selectively activates Ras-Raf-MEK-ERK and p38 as well as JNK signaling in Huh7 cells; p38 and JNK signaling in FL83B; Ras-Raf-MEK-ERK in HepG2 cells; and p38 activation in Hep3B cells, while OA only induced a moderate Ras activity in Huh 7 and HepG2 cells. The wide and broad effect of UA in different signaling pathways may explain why UA has a higher efficiency than OA in the inhibition of the process related to tumor development. The results suggest that three separate MAPK signaling pathways selectively participate in the UA-mediated activities in the reversal of HBx-induced carcinogenic mechanisms.

In our previous study, we demonstrated that HBx expression elicits a migration response in Huh7 hepatoma cells, which is associated with MMP-3.²² The findings suggest that MMP-3 plays a central role in the hepatoma cell locomotion process. In this study, we demonstrated that UA and OA could prevent tumor formation and lowered the liver damage induced by HBV-containing hepatoma cells. We identified that MAPK signaling pathways selectively participate in the prevention process in the reversal of HBx-induced carcinogenic mechanisms in different hepatoma cells. Preintra-peritoneal injection of UA fully prevented tumor growth of HBV-containing 2.2.15 cells, while OA-treated mice had smaller tumors than the control group. The most important finding of this study was that UA treatment has a similar inhibitive effect to silymarin, whose preventive activity has been demonstrated in a HBx transgenic mouse model.³⁶ The levels of GOT, GPT, BUN and CRE in the UA- and OA-treated mice were comparable with those of the negative controls, suggesting that UA and OA have an effect against HBx-mediated tumorigenic activities and were without toxicity in a mouse model. Although UA and OA have been demonstrated to be useful antitumor reagents in many studies, the current study suggests that UA and OA may be useful agents against hepatocellular carcinoma in clinical practice in the future.

In this study we used UA and OA at a concentration of 9 μ M, which showed biological activity without a toxic effect for *in vitro*

experiments. Regarding higher concentrations, cells treated with 15 μM UA demonstrated approximately 25% cell death at 24 h post-treatment, while cells treated with 20 μM UA or OA exhibited even more significant cell death. Although certain signaling molecules also revealed phosphorylation in the cells treated with higher concentrations of UA or OA, we focused on their effects at a nontoxic dosage in this study. For *in vivo* study, we tested 50 mg/kg and 200 mg/kg dosages of UA or OA in animal experiments, which both showed tumor preventive activity. However, no dose-dependent effect was seen in the animal study. The findings of this study suggest that a low dosage of 50 mg/kg of UA or OA has an effective antitumor activity in a mouse model *in vivo*.

We have shown that UA and OA are able to reverse HBx-mediated transcriptional activation, hepatoma cell migration and TGF- β -induced apoptosis, UA having a better activity than OA. We also identified the signaling mechanisms involved: p38 signaling plays a critical role in UA-mediated activity, while the JNK pathway is also involved; in addition, ERK signaling has an important role in the cell migration of hepatoma cells, and UA could prevent tumor formation and lower the liver damage induced by HBV-containing hepatoma cells. As long-term daily use of UA does not affect liver and renal function, there exists the potential for the development of UA as a therapeutic agent for the treatment of liver cancer.

AUTHOR INFORMATION

Corresponding Author

*Graduate Institute of Biotechnology, National Pingtung University of Science and Technology, 1, Shuefu Rd., Neipu, Pingtung, 91201, Taiwan. Phone: 886-8-7703202 ext 5192. Fax: 08-7740550. E-mail: wlshih@mail.npust.edu.tw.

Funding Sources

This work was supported by a grant from the National Science Council of Taiwan (NSC 98-2313-B-020-004-MY3).

ACKNOWLEDGMENT

We thank Sarah Parkin for copy-editing the manuscript.

REFERENCES

- (1) Arbutnot, P.; Kew, M. Hepatitis B virus and hepatocellular carcinoma. *Int. J. Exp. Pathol.* **2001**, *82* (2), 77–100.
- (2) Francis, D. P. Hepatitis B virus vaccine. An opportunity for control. *JAMA, J. Am. Med. Assoc.* **1983**, *250* (14), 1891–2.
- (3) Yim, H. J. Hepatitis B virus genetic diversity and mutant. *Korean J. Hepatol.* **2008**, *14* (4), 446–64.
- (4) Xu, Z.; Liu, Y.; Xu, T.; Chen, L.; Si, L.; Wang, Y.; Ren, X.; Zhong, Y.; Zhao, J.; Xu, D. Acute hepatitis B infection associated with drug-resistant hepatitis B virus. *J. Clin. Virol.* **2010**, *48* (4), 270–4.
- (5) Nystrom, J.; Cardell, K.; Bjornsdottir, T. B.; Fryden, A.; Hultgren, C.; Sallberg, M. Improved cell mediated immune responses after successful re-vaccination of non-responders to the hepatitis B virus surface antigen (HBsAg) vaccine using the combined hepatitis A and B vaccine. *Vaccine* **2008**, *26* (47), 5967–72.
- (6) Benhenda, S.; Cougot, D.; Buendia, M. A.; Neuveut, C. Hepatitis B virus X protein molecular functions and its role in virus life cycle and pathogenesis. *Adv. Cancer Res.* **2009**, *103*, 75–109.
- (7) Xu, Z.; Yen, T. S.; Wu, L.; Madden, C. R.; Tan, W.; Slagle, B. L.; Ou, J. H. Enhancement of hepatitis B virus replication by its X protein in transgenic mice. *J. Virol.* **2002**, *76* (5), 2579–84.
- (8) Zhang, X.; Zhang, H.; Ye, L. Effects of hepatitis B virus X protein on the development of liver cancer. *J. Lab. Clin. Med.* **2006**, *147* (2), 58–66.
- (9) Cragg, G. M.; Grothaus, P. G.; Newman, D. J. Impact of natural products on developing new anti-cancer agents. *Chem. Rev.* **2009**, *109* (7), 3012–43.
- (10) Reddy, L.; Odhav, B.; Bhoola, K. D. Natural products for cancer prevention: a global perspective. *Pharmacol. Ther.* **2003**, *99* (1), 1–13.
- (11) Liu, J. Pharmacology of oleanolic acid and ursolic acid. *J. Ethnopharmacol.* **1995**, *49* (2), 57–68.
- (12) Ramos, A. A.; Pereira-Wilson, C.; Collins, A. R., Protective effects of Ursolic acid and Luteolin against oxidative DNA damage include enhancement of DNA repair in Caco-2 cells. *Mutat. Res.* **2010**.
- (13) Tsai, S. J.; Yin, M. C. Antioxidative and anti-inflammatory protection of oleanolic acid and ursolic acid in PC12 cells. *J. Food Sci.* **2008**, *73* (7), H174–8.
- (14) Wang, X.; Li, L.; Wang, B.; Xiang, J. Effects of ursolic acid on the proliferation and apoptosis of human ovarian cancer cells. *J. Huazhong Univ. Sci. Technol., Med. Sci.* **2009**, *29* (6), 761–4.
- (15) Kanjoormana, M.; Kuttan, G. Antiangiogenic activity of ursolic acid. *Integr. Cancer Ther.* **2010**, *9* (2), 224–35.
- (16) Zhang, Y. X.; Kong, C. Z.; Wang, L. H.; Li, J. Y.; Liu, X. K.; Xu, B.; Xu, C. L.; Sun, Y. H. Ursolic acid overcomes Bcl-2-mediated resistance to apoptosis in prostate cancer cells involving activation of JNK-induced Bcl-2 phosphorylation and degradation. *J. Cell. Biochem.* **2010**, *109* (4), 764–73.
- (17) Huang, H. C.; Huang, C. Y.; Lin-Shiau, S. Y.; Lin, J. K. Ursolic acid inhibits IL-1 β or TNF- α -induced C6 glioma invasion through suppressing the association ZIP/p62 with PKC- ζ and down-regulating the MMP-9 expression. *Mol. Carcinog.* **2009**, *48* (6), 517–31.
- (18) Manu, K. A.; Kuttan, G. Ursolic acid induces apoptosis by activating p53 and caspase-3 gene expressions and suppressing NF- κ B mediated activation of bcl-2 in B16F-10 melanoma cells. *Int. Immunopharmacol.* **2008**, *8* (7), 974–81.
- (19) Pathak, A. K.; Bhutani, M.; Nair, A. S.; Ahn, K. S.; Chakraborty, A.; Kadara, H.; Guha, S.; Sethi, G.; Aggarwal, B. B. Ursolic acid inhibits STAT3 activation pathway leading to suppression of proliferation and chemosensitization of human multiple myeloma cells. *Mol. Cancer Res.* **2007**, *5* (9), 943–55.
- (20) Zhang, Y.; Jayaprakasam, B.; Seeram, N. P.; Olson, L. K.; DeWitt, D.; Nair, M. G. Insulin secretion and cyclooxygenase enzyme inhibition by cabernet sauvignon grape skin compounds. *J. Agric. Food Chem.* **2004**, *52* (2), 228–33.
- (21) Shih, W. L.; Kuo, M. L.; Chuang, S. E.; Cheng, A. L.; Doong, S. L. Hepatitis B virus X protein inhibits transforming growth factor- β -induced apoptosis through the activation of phosphatidylinositol 3-kinase pathway. *J. Biol. Chem.* **2000**, *275* (33), 25858–64.
- (22) Yu, F. L.; Liu, H. J.; Lee, J. W.; Liao, M. H.; Shih, W. L. Hepatitis B virus X protein promotes cell migration by inducing matrix metalloproteinase-3. *J. Hepatol.* **2005**, *42* (4), 520–7.
- (23) Zelivinski, S.; Spellman, M.; Kellerman, M.; Kakitelashvili, V.; Zhou, X. W.; Lugo, E.; Lee, M. S.; Taylor, R.; Davis, T. L.; Hauke, R.; Lin, M. F. ERK inhibitor PD98059 enhances docetaxel-induced apoptosis of androgen-independent human prostate cancer cells. *Int. J. Cancer* **2003**, *107* (3), 478–85.
- (24) Nakaya, K.; Oishi, R.; Funaba, M.; Murakami, M. A JNK inhibitor SP600125 induces defective cytokinesis and enlargement in P19 embryonal carcinoma cells. *Cell Biochem. Funct.* **2009**, *27* (7), 468–72.
- (25) Su, J.; Cui, X.; Li, Y.; Mani, H.; Ferreyra, G. A.; Danner, R. L.; Hsu, L. L.; Fitz, Y.; Eichacker, P. Q. SB203580, a p38 inhibitor, improved cardiac function but worsened lung injury and survival during Escherichia coli pneumonia in mice. *J. Trauma* **2010**, *68* (6), 1317–27.
- (26) Crocenzi, F. A.; Roma, M. G. Silymarin as a new hepatoprotective agent in experimental cholestasis: new possibilities for an ancient medication. *Curr. Med. Chem.* **2006**, *13* (9), 1055–74.
- (27) Jiao, J.; Cao, H.; Chen, X. W.; Zhou, M. J.; Liu, Z. H.; Ding, Z. H. Downregulation of HBx mRNA in HepG2.2.15 cells by small interfering RNA. *Eur. J. Gastroenterol. Hepatol.* **2007**, *19* (12), 1114–8.

(28) Doong, S. L.; Tsai, C. H.; Schinazi, R. F.; Liotta, D. C.; Cheng, Y. C. Inhibition of the replication of hepatitis B virus in vitro by 2',3'-dideoxy-3'-thiacytidine and related analogues. *Proc. Natl. Acad. Sci. U.S.A.* **1991**, *88* (19), 8495–9.

(29) Lin, J. D.; Lin, P. Y.; Chen, L. M.; Fang, W. H.; Lin, L. P.; Loh, C. H. Serum glutamic-oxaloacetic transaminase (GOT) and glutamic-pyruvic transaminase (GPT) levels in children and adolescents with intellectual disabilities. *Res. Dev. Disabil.* **2010**, *31* (1), 172–7.

(30) Kawaida, K.; Matsumoto, K.; Shimazu, H.; Nakamura, T. Hepatocyte growth factor prevents acute renal failure and accelerates renal regeneration in mice. *Proc. Natl. Acad. Sci. U.S.A.* **1994**, *91* (10), 4357–61.

(31) Clippinger, A. J.; Gearhart, T. L.; Bouchard, M. J. Hepatitis B virus X protein modulates apoptosis in primary rat hepatocytes by regulating both NF-kappaB and the mitochondrial permeability transition pore. *J. Virol.* **2009**, *83* (10), 4718–31.

(32) Kim, S. Y.; Kim, J. K.; Kim, H. J.; Ahn, J. K. Hepatitis B virus X protein sensitizes UV-induced apoptosis by transcriptional transactivation of Fas ligand gene expression. *IUBMB Life* **2005**, *57* (9), 651–8.

(33) Zhang, Y.; Kong, C.; Zeng, Y.; Wang, L.; Li, Z.; Wang, H.; Xu, C.; Sun, Y. Ursolic acid induces PC-3 cell apoptosis via activation of JNK and inhibition of Akt pathways in vitro. *Mol. Carcinog.* **2010**, *49* (4), 374–85.

(34) Es-Saady, D.; Najid, A.; Simon, A.; Denizot, Y.; Chulia, A. J.; Delage, C. Effects of Ursolic Acid and its Analogues on Soybean 15-Lipoxygenase Activity and the Proliferation Rate of A human Gastric Tumour Cell Line. *Mediators Inflammation* **1994**, *3* (3), 181–4.

(35) Shan, J. Z.; Xuan, Y. Y.; Zheng, S.; Dong, Q.; Zhang, S. Z. Ursolic acid inhibits proliferation and induces apoptosis of HT-29 colon cancer cells by inhibiting the EGFR/MAPK pathway. *J. Zhejiang Univ. Sci. B* **2009**, *10* (9), 668–74.

(36) Wu, Y. F.; Fu, S. L.; Kao, C. H.; Yang, C. W.; Lin, C. H.; Hsu, M. T.; Tsai, T. F. Chemopreventive effect of silymarin on liver pathology in HBV X protein transgenic mice. *Cancer Res.* **2008**, *68* (6), 2033–42.